

Theoretical Studies of Solid–Liquid Interfaces: Molecular Interactions at the MgO(001)–Water Interface

Michael A. Johnson, Eugene V. Stefanovich, and Thanh N. Truong*

Henry Eyring Center for Theoretical Chemistry, Department of Chemistry, University of Utah, Salt Lake City, Utah 84112

Received: March 6, 1998; In Final Form: June 1, 1998

We have applied a novel theoretical and computational method called CECILIA (combined embedded cluster at the interface with liquid approach) to study adsorption of molecular water on the MgO(001) surface and its interface with water. The MgO(001) surface is modeled by a quantum cluster embedded in a field of pseudopotentials and point charges. The effects of an aqueous environment are included by placing a dielectric continuum in the region above the embedded cluster. Calculated geometry, energetics, and electronic spectra for adsorbed water are in good agreement with available experimental and theoretical data. In particular, many features of the interfacial structure and dynamics (McCarthy, M. I.; Schenter, G. K.; Scamehorn, C. A.; Nicholas, J. B. *J. Phys. Chem.* **1996**, *100*, 16989) are well-reproduced in our calculations. These results demonstrate the suitability of the CECILIA model for studying chemical processes at solid–liquid interfaces.

Introduction

Ion sorption and chemical reactions at solid–liquid interfaces are central features in many natural and industrial processes. Examples include transportation of groundwater contaminants, electrode phenomena, corrosion, and catalysis. For geochemistry and atmospheric chemistry, surfaces of metal oxides are of particular interest as these compounds are major components of rocks, soils, and airborne dust particles. In addition, metal oxides often exhibit significant catalytic activity.

Under natural conditions, surfaces of metal oxides are often found in contact with water. The solid–liquid interface can be formed when oxides are immersed in bulk water or when several monolayers of water adsorb from a humid atmosphere. For many oxides it has been found that water molecules dissociate upon contact with the surface, forming various types of surface hydroxyl groups. It is also well-established that these hydroxyl groups play a decisive role in all chemical properties of oxide surfaces, including ion sorption, dissolution, and catalytic activity.¹

Initially, model approaches based on bond valence analysis have been used to estimate stabilities of interfacial hydroxyl groups.^{2–6} Recently, classical molecular mechanical models appeared which can address the structural properties of interfaces at an atomistic level.^{7–10} For an accurate description of quantum effects in bond breaking and bond forming processes, i.e., chemical reactions at interfaces, ab initio methods of quantum chemistry are needed. A few quantum mechanical calculations concerning the properties of water and hydroxyl groups on oxide surfaces have been performed using either periodic boundary conditions^{11–15} or the molecular cluster model (for some recent examples, see refs 16–18). Only limited attempts have been made to include solvent effects in theoretical studies of chemical reactivity at the oxide–liquid interface. For example, in several studies,^{19–21} the binding energy of a water molecule at the

SiO₂–water interface was simply estimated as the binding energy at the bare surface minus the binding energy of the water dimer.

In our previously published article²² (referred to in this paper as article 1) we have suggested a model, called CECILIA (combined embedded cluster at the interface with liquid approach), with the ability to study chemical processes at solid–liquid interfaces. In this approach, an embedded cluster model is used to represent adsorbate interactions with the solid surface, and a dielectric continuum is used in the region above the cluster to provide solvent effects. We presented a thorough analysis of interactions involving various adsorbates (Na⁺, Cl[−], NaCl, H₂O) with the NaCl(001)–vacuum and NaCl(001)–water interfaces. It was concluded that the presence of bulk water significantly changes geometries and energetics of adsorbed species.

Although results from our initial study of the NaCl–water interface are very encouraging, without extensive comparison to experimental observations and independent theoretical studies, there remains some uncertainty with regard to the usefulness of the CECILIA model. Therefore, the main motivation for the present work is to further confirm the utility of the CECILIA method. For this study, the MgO–water system provides a good test case due to existing experimental and theoretical data. In particular, numerous ab initio cluster and embedded cluster calculations^{16,23–26} have established the applicability of these methods for studying reactivity of MgO surfaces. Moreover, a great deal of experience has been accumulated in dielectric continuum modeling of chemical processes in bulk water.^{27–36} These developments suggest that a combination of these two approaches in the CECILIA model would result in a useful tool for studying reactivity at MgO–water interfaces. Unfortunately, there are very few reliable experimental and rigorous theoretical results on MgO–water interfaces available for comparison to, and testing the accuracy of, the CECILIA model. Of special interest for this purpose are the results obtained in the most comprehensive simulations, to date, of the structure and dynamics at the MgO–water interface performed by McCarthy

* Corresponding author.

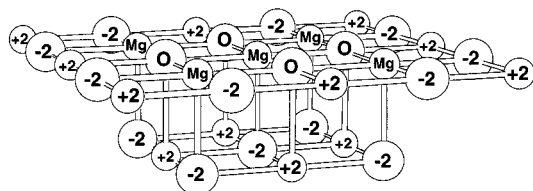


Figure 1. Cluster model of the MgO(001) surface. This cluster is embedded in the field generated by 222 additional point charges (not shown).

et al.³⁷ In these simulations, the SPC³⁸ representation of water was used in simulation cells of 64 and 128 water molecules. The SPC model predicts a dielectric constant of 68 for water at 300 K.³⁹ Since electrostatic solvent effects scale as $(\epsilon - 1)/\epsilon$, this simple point charge model can yield 99% of the solvent polarization. The simulations were based on a 2-D periodic boundary condition, and electrostatic interactions were summed using the Ewald method. This classical molecular dynamics and Monte Carlo study used intermolecular potentials that were fit to correlation-corrected periodic Hartree-Fock (PHF) calculations for various water-surface orientations; thus near-surface forces were taken into account. These potentials remained unperturbed throughout the simulation. This is common practice when studying systems in which the breaking and formation of covalent bonds are not significant. For example, classical potentials have been successfully applied to the study of both MgO crystal surfaces and liquid water.⁴⁰⁻⁴⁷ However, results from our recent study⁴⁸ of interactions at the MgO-water interface predict that dissociated water has a lower total energy than water adsorbed in the molecular form. Thus, strictly speaking, potentials of the type $\text{Mg}^{2+}-\text{H}_2\text{O}$, $\text{O}^{2-}-\text{H}_2\text{O}$, and $\text{H}_2\text{O}-\text{H}_2\text{O}$, cannot sufficiently describe the interfacial chemistry. Nevertheless, we believe that energy minima corresponding to molecular and dissociated water are separated by some activation barrier, so that molecular adsorption has the meaning, at least, as a metastable state. Thus the results of MD simulations are useful only in this limited sense. These results can be compared to the predictions of the quantum mechanical CECILIA model if, in the latter, we restrict ourselves to the local energy minimum corresponding to the molecular form of adsorbed water. MD simulations³⁷ predict that molecular water forms a structured layer near the MgO-water interface. Water molecules can diffuse rather freely within this layer; however, exchange with bulk water is suppressed. These fine details of the interfacial structure and dynamics can serve as a critical test of our CECILIA method. In this paper, we will demonstrate that our CECILIA model does indeed yield such features. In particular, the calculated energy profile for molecular water desorption from the MgO-water interface gives a simple explanation for the results of molecular mechanics simulations.

Computational Method

The theoretical model employed in this study is similar to that used in article 1. The main feature of the CECILIA method is the combination of an embedded cluster model^{25,49} for representing interactions of the surface active site with the crystal lattice and the use of a dielectric continuum to model long-range polarization of the solvent. We used the cluster shown in Figure 1 to model the MgO(001) surface. For computational feasibility, ionic cores were approximated by effective core pseudopotentials (ECP).⁵⁰ We used the standard valence CEP-31++G** basis set on the atoms of the water molecule. The CEP-31G* basis set was used on the four oxygen ions (labeled

"O") nearest to the central Mg ion. Oxygen ions marked as "-2" in Figure 1 were modeled as point charges ($q_0 = -2$) without basis functions. The CEP-31G basis set was placed on the five Mg ions at the surface (labeled "Mg"); other Mg ions in the cluster (labeled "+2") were approximated by bare pseudopotentials without basis sets. In order to represent the rest of the crystal, the cluster described above was embedded in the field generated by 222 lattice point charges of ± 2 (not shown in Figure 1) so that the entire system (cluster + point charges) consisted of four stacked 8×8 layers resulting in an $8 \times 8 \times 4$ slab. This finite lattice has been shown to provide an accurate Madelung potential at the (001) rock salt crystal surface.^{22,49} An accurate representation of the Madelung field largely eliminates a dependence of results on cluster size. It has been shown²⁴ that changing the cluster size from 10 to 18 atoms results in a binding energy that differs by less than 0.5 kcal/mol for molecular water adsorption. Thus, using a cluster of nine ions in the present study is justified. We also do not expect that neglect of the crystal lattice polarization beyond boundaries of the quantum cluster could significantly affect our results. A recent ab initio study of H_2O adsorption at an aluminum impurity site on the MgO(001) surface²⁶ suggests that polarization corrections to reaction energies do not exceed 2 kcal/mol (see also ref 51).

In the CECILIA approach, a self-consistent treatment of the solvent polarization is achieved by using the generalized conductor-like screening model (GCOSMO)²⁸⁻³⁴ in which the liquid is represented as a dielectric continuum separated from the solute (in our case, crystal surface and adsorbate) by a sharp boundary. Cavities for CECILIA calculations were constructed using the GEPOL93 algorithm⁵² as a set of interlocking spheres centered on nuclei. Atomic radii for cavity construction were taken from our previous work: 1.172 Å for H; 1.576 Å for O.³¹ The atomic radius for Mg (1.431 Å) was fitted to the experimental hydration free energy of the Mg^{2+} ion (-455.5 kcal/mol⁵³). We used a solvent-excluding surface,⁵² and the cavity boundary was truncated so that only adsorbed atoms and surface ions of Figure 1 were solvated. Extension of the cavity to cover surface sites farther from the cluster does not change the electronic structure and energetics of surface reactions. The solvent polarization field is represented in a boundary element approach as a set of point charges on the cavity (60 charges per each complete atomic sphere) determined self-consistently with the charge density distribution of the solute. An important advantage of the GCOSMO solvation model is that the polarization potential is included directly in the Fock matrix as a nonlinear functional depending on the density matrix of the cluster. Thus, self-consistency is achieved in a single SCF run. Dispersion-repulsion contributions to the solvation free energy were calculated using Floris and Tomasi's method,⁵⁴ in conjunction with OPLS force field parameters.⁴⁵ Cavitation energy was calculated using a method suggested by Pierotti⁵⁵ and Huron and Claverie.⁵⁶

Geometry optimizations using analytical energy gradients²⁹ were performed using the restricted Hartree-Fock (RHF) approximation. Reported energies include correlation corrections which were estimated by performing single-point second order Møller-Plesset perturbation theory (MP2) calculations at RHF optimized geometries. Such practice may result in about 1 kcal/mol error as compared to full MP2 optimization.¹⁶ In the energy minimization procedures, all adsorbate atoms were fully relaxed with no elements of symmetry assumed. As noted in the Introduction, in this paper we are concerned with the interfacial properties of molecular (not dissociated) water.

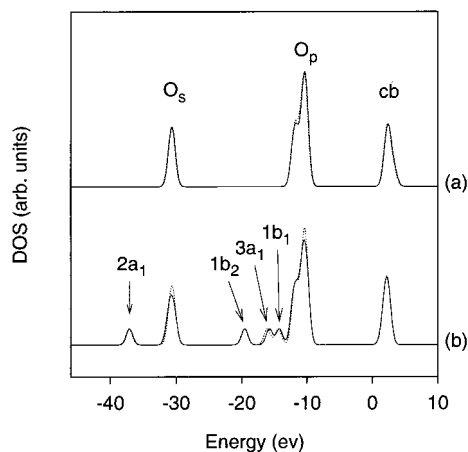


Figure 2. Comparison of DOS in vacuum (solid line) and in the hydrated state (dotted line). The conduction band states are labeled “cb”. (a) MgO(001) surface. (b) Water adsorbed on MgO(001).

Therefore, reported results refer to the local minimum corresponding to molecular H₂O. All surface ions were held fixed at ideal lattice positions. This is a reasonable approximation since reconstruction of the MgO(001) surface is known to be minimal,⁵⁷ and a recent study⁵⁸ suggests that we may gain about 3 kcal/mol in adsorption energy by relaxing surface ions.

In characterizing the surface electronic structure of cluster and adsorbed water configurations considered in this work, we present results for the electronic density of states (DOS). This information can be useful for qualitative analysis of data collected in electron spectroscopy experiments.^{59–63} As suggested earlier,⁶⁰ to attain the best agreement between calculated density of states and experimental UPS and MIES spectra for MgO, our DOS graphs were generated by smoothing of orbital energy levels with Gaussian functions having a width of 1.0 eV at half-maximum.

All calculations were performed using our locally modified GAUSSIAN92/DFT computer code.⁶⁴

Results and Discussion

In Figure 2a we show the calculated density of states for the MgO(001) surface in both vacuum and aqueous environments. Our calculated DOS of a bare MgO(001) surface agrees well with that from periodic HF studies.⁶⁵ The spectrum of occupied levels consists of two bands separated by about 20 eV. The higher energy band with binding energies of approximately 10 eV is composed primarily of oxygen p-orbitals (O_p). The experimental width of the O_p band, taken from UPS spectra,^{60,61} is about 6 eV. Because our quantum cluster consists entirely of surface atoms, and bulk atoms are known to contribute to the bottom of the valence band,⁶⁰ our calculated O_p band is only 4 eV wide. In agreement with the high ionicity of the MgO(001) surface, Mulliken population analysis yields a charge on oxygen ions of -1.69 . Thus, our embedded molecular cluster provides a good representation of the basic features of the MgO(001) surface electronic structure. This gives us confidence that reactive properties of the MgO(001) surface and the MgO(001)–water interface will be well-reproduced in adsorption calculations.

In the presence of liquid water modeled as a dielectric continuum, the electronic structure of the MgO cluster does not change much (see dotted line in Figure 2a). Due to positive values of the solvent polarization field on surface oxygen ions, occupied energy levels shift slightly (by about 0.07 eV) to higher

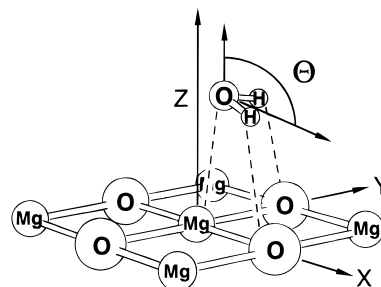


Figure 3. Optimized geometry for water at the MgO(001)–vacuum interface. Numerical parameters for both the vacuum and water interfaces are listed in Table 1.

TABLE 1: Structure (Å, deg) and MP2 Adsorption Energy (kcal/mol) for a Water Molecule at the MgO(001) Vacuum and Aqueous Interface

param ^a	vacuum interface	aqueous interface
O–H bond length	0.954	0.956
H–O–H angle	105.35	105.30
O _z	2.32 (2.02) ^b	2.31 (2–3) ^b
O _x = O _y	0.30 (0.54) ^b	0.32
tilt angle θ	106.7 (105) ^b	110.0 (107 or 60) ^b
binding energy	+14.2 (+17.3) ^b	–1.8

^a See Figure 3. ^b Calculated in ref 37.

electron binding energies. This shift is accompanied by a slight increase of surface ionicity (oxygen charges of -1.71).

The optimized geometry for molecular water adsorption on the MgO(001) surface is shown in Figure 3, and numerical parameters are listed in Table 1. In agreement with previous periodic Hartree–Fock calculations,^{37,51} water oxygen binds to the lattice magnesium ion, and the molecular symmetry axis is tilted by about 106.7 degrees with respect to the surface normal so that water hydrogens form hydrogen bonds with lattice oxygen ions (bond distance 2.33 Å). This near-planar configuration of adsorbed water is also consistent with polarization FTIR⁶⁶ and RAIRS⁶⁷ experiments. The calculated binding energy of water at the clean MgO(001) surface (14.2 kcal/mol) agrees well with a number of experimental estimates ranging from 10 to 19 kcal/mol.^{67–71} This is also consistent with results of ab initio periodic Hartree–Fock³⁷ (17.3 kcal/mol) and other embedded cluster²⁴ (14.3–14.8 kcal/mol) calculations. Molecularly adsorbed water induces additional DOS peaks below O_{2p} and O_{2s} valence bands. In Figure 2b, these features are labeled according to molecular orbitals on the water molecule. The relative positions of the O_{2p}, 1b₂, 3a₁, and 1b₁ peaks are in good agreement with recent MIES and UPS spectra of a D₂O-covered MgO(001) surface⁵⁹ (see also ref 61).

The average structure of H₂O adsorbed at the MgO–water interface (see Table 1) is slightly different from that at the MgO–vacuum interface. The noticeable difference is an increase in the tilt angle by 3.3°. This is in reasonable agreement with calculations by McCarthy et al.³⁷ who found that in going from the MgO–vacuum to the MgO–water interface, the tilt angle changes from 105 to 107°. In this study, we were not able to reproduce another configuration corresponding to the tilt angle of 60° as observed in the angular distribution of near-surface water molecules.³⁷ This orientation probably appears as a result of cooperative interactions of several water molecules that were not included in our model. The DOS for water adsorption at the MgO–water interface is nearly identical to adsorption on the dry MgO surface (see the dotted line in Figure 2b).

Next, we studied the energy profile for water desorption from the interface E_{total}(O₂) (solid line in Figure 4a). In these

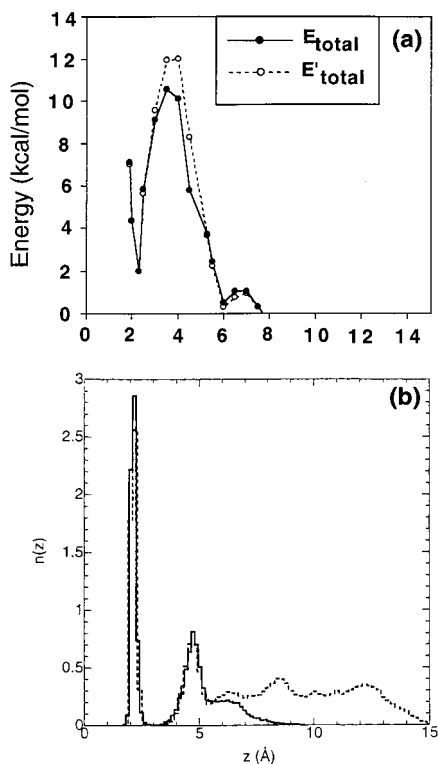


Figure 4. Characteristics of the MgO(001)–water interface as functions of distance (z) between water oxygens and the surface plane. (a) Energy profile ($E_{\text{total}}(\text{O}_z)$) for a water molecule adsorbed at the interface calculated using the CECILIA model. (b) Density profiles previously obtained from molecular dynamics simulations (reproduced with permission from ref 37).

calculations the reaction coordinate was the height of the water oxygen above the surface (O_z). The lateral position of oxygen was fixed to be the same as in the minimum energy configuration ($\text{O}_x = \text{O}_y = 0.32 \text{ \AA}$), while the positions of hydrogen atoms were allowed to relax. It is interesting to note that the energy of H_2O adsorbed at the interface is 1.8 kcal/mol higher than that for H_2O in bulk liquid. Thus, the adsorbed state corresponds to a local minimum on the free energy surface. To desorb from the interface, the water molecule should overcome a rather high barrier of about 9 kcal/mol.

Owing to the simplicity and physically transparent formulation of the CECILIA model, we can perform a detailed analysis of the various contributions to the energy profile of Figure 4a. One can represent the interfacial adsorption in terms of three mutually interacting systems: water molecule, crystal surface, and liquid. Assuming that the total interaction energy is additive, we can write

$$E'_{\text{total}}(\text{O}_z) = E_{\text{H}_2\text{O}-\text{surface}}(\text{O}_z) + E_{\text{H}_2\text{O}-\text{liquid}}(\text{O}_z) + E_{\text{surface}-\text{liquid}}(\text{O}_z) \quad (1)$$

The three individual contributions to $E'_{\text{total}}(\text{O}_z)$ can be estimated from the three separate calculations. In each of these calculations we fixed the geometry of the water molecule to be the same as in the case of $E_{\text{total}}(\text{O}_z)$. The three interaction curves, as well as the sum represented by $E'_{\text{total}}(\text{O}_z)$ above, are shown in Figure 5.

For $E_{\text{H}_2\text{O}-\text{surface}}(\text{O}_z)$ we calculated the energy profile for molecular water desorption from the bare MgO surface represented by the embedded cluster without the dielectric continuum present. This gives a familiar interaction curve with a deep minimum of -14 kcal/mol .

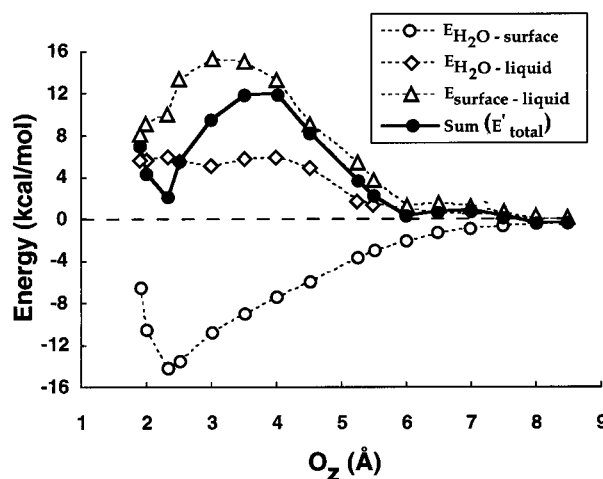


Figure 5. Total interaction energy (solid line) of a water molecule at the MgO–water interface as the sum of three distinct interactions (see eq 1).

For $E_{\text{H}_2\text{O}-\text{liquid}}(\text{O}_z)$, the crystal lattice was removed while the dielectric cavity surrounding the surface atoms (at a distance of 1.4–1.6 \AA from the crystal surface) and the water molecule remained. This type of calculation resembles the situation that exists when a water molecule penetrates into bulk liquid through the liquid–gas interface. Energy gradually decreases as H_2O penetrates deeper into the bulk liquid.

The curve for $E_{\text{surface}-\text{liquid}}(\text{O}_z)$ was obtained in calculations where the water molecule was absent, but the shape of the dielectric cavity above the MgO surface was the same as if the water molecule were present. This plot represents changes in hydration energy of the MgO surface cluster as the shape of the hydration cavity varies in the process of H_2O desorption. $E_{\text{surface}-\text{liquid}}(\text{O}_z)$ has a broad maximum extending from 2 to 6 \AA outward from the crystal surface. This barrier originates from a reduction in electrostatic hydration of the MgO surface and a larger cavitation energy due to the increased size of the dielectric cavity when a water molecule moves away from the surface.

As seen in Figure 4a, the sum of the three energy components (shown as a broken line) indeed serves as a good approximation to the total interaction energy at the MgO–water interface. At small values of O_z ($\leq 2 \text{ \AA}$), the leading contribution comes from the repulsive part of the $E_{\text{H}_2\text{O}-\text{surface}}(\text{O}_z)$ interaction. $E_{\text{surface}-\text{liquid}}(\text{O}_z)$ is largely responsible for the energy barrier on the $E_{\text{total}}(\text{O}_z)$ curve. Existence of this barrier prevents water molecules in the first adsorbed layer from exchanging freely with bulk water. A low probability of such interchange events was observed in molecular dynamics simulations.³⁷ However, our interpretation of this effect is different from that given by McCarthy and co-workers.³⁷ They suggested that water molecules are confined to the interface due to the strong water–surface attraction. In contrast, we see from Figure 5 that, due to the combined repulsive effect of $E_{\text{H}_2\text{O}-\text{liquid}}(\text{O}_z)$ and $E_{\text{surface}-\text{liquid}}(\text{O}_z)$, the location of a water molecule at 2.3 \AA from the crystal surface corresponds to a local minimum whose energy is 1.8 kcal/mol higher than that of a water molecule in the bulk liquid.

From the analysis above it follows that energy profiles for other lateral positions of adsorbed water (as well as the energy profile averaged over O_x and O_y) will be qualitatively similar to that presented in Figure 4a. This allows us to conclude that the average density of water molecules near the interface should anticorrelate with the energy plot in Figure 4a; i.e., minima on the energy plot correspond to maximum density of particles and

maxima on the energy plot indicate regions more likely to be void of water molecules. Such behavior is clearly seen from comparison of Figure 4a with the plot in Figure 4b, where we have reproduced the density profile for water molecules near the MgO surface obtained in molecular dynamics simulations.³⁷ The local energy minimum at 2.3 Å corresponds to a narrow sharp density peak at oxygen–surface distances of 2–2.5 Å. The energy barrier at 3–4 Å corresponds to the gap in the density profile at $O_z = 3-4$ Å. Even a shallow energy minimum at about 6 Å seems to have a counterpart in the density maximum at 5 Å (second water layer). Both profiles of Figure 4 indicate a homogeneous phase of water exists beyond 7 Å of the MgO(001) surface. Although there is some quantitative discrepancy, the overall qualitative agreement between the free energy profile from CECILIA calculations and the water density profile from molecular dynamics simulations is remarkable.

Conclusions

Using an ab initio embedded cluster model, we have systematically examined the structure and energetics of water adsorption on the MgO(001) surface and at the MgO(001)–water interface. Comparison of our results with previous experimental and theoretical studies strongly suggests that the CECILIA model is a reliable and cost-effective tool for studying chemical processes at solid–liquid interfaces. Of particular interest is a remarkable qualitative agreement between the energy profile for a single water molecule interacting with the MgO–water interface obtained using the CECILIA model and the interfacial density profile predicted by molecular dynamics simulations.³⁷ This agreement indicates that a continuum representation of the solvent can reasonably model complicated many-body interactions at solid–liquid interfaces.

This study further confirms the applicability of the CECILIA approach in modeling solid–liquid processes, particularly of molecular water adsorption on MgO. We can now turn our attention to the more challenging problem regarding chemical reactivity of oxide–water interfaces. In our most recent calculations,⁴⁸ we have identified a low-energy minimum for water adsorption at the MgO(001)–water interface (about 13 kcal/mol lower than adsorbed molecular H₂O). It involves heterolytic dissociative chemisorption of water to form surface hydroxyl groups that are stabilized by solvent polarization. This result is consistent with the experimentally observed dissolution of the MgO(001) surface and with the spontaneous transformation of MgO (periclase) to the MgO(OH)₂ crystal (brucite) in the presence of liquid water. The full results of these calculations will be published in a forthcoming paper.

Acknowledgment. This research was supported by the National Science Foundation through a NSF Young Investigator Award to T.N.T. We are thankful to Prof. V. Kemper for sending his manuscript⁵⁹ prior to publication.

References and Notes

- Boehm, H.-P.; Knözinger, H. *Catalysis: Science and Technology*; Springer-Verlag: Berlin, Heidelberg, New York, 1983; Vol. 4, p 39.
- Hiemstra, T.; Riemsdijk, W. H. V.; Bolt, G. H. *J. Colloid Interface Sci.* **1989**, *133*, 91.
- Hiemstra, T.; Venema, P.; Riemsdijk, W. H. V. *J. Colloid Interface Sci.* **1996**, *184*, 680.
- Sverjensky, D. A.; Sahai, N. *Geochim. Cosmochim. Acta* **1996**, *60*, 3773.
- Parks, G. A. *Chem. Rev.* **1965**, *65*, 177.
- Bargar, J. R.; Towle, S. N.; Brown, G. E., Jr.; Parks, G. A. *J. Colloid Interface Sci.* **1997**, *185*, 473.
- Rustad, J. R.; Felmy, A. R.; Hay, B. P. *Geochim. Cosmochim. Acta* **1996**, *60*, 1553.
- Boek, E. S.; Coveney, P. V.; Skipper, N. T. *J. Am. Chem. Soc.* **1995**, *117*, 12608.
- Skipper, N. T.; Refson, K.; McConnell, J. D. C. *J. Chem. Phys.* **1991**, *94*, 7434.
- Delville, A. *Langmuir* **1992**, *8*, 1796.
- Goniakowski, J.; Gillan, M. J. *Surf. Sci.* **1996**, *350*, 145.
- Fahmi, A.; Minot, C. *Surf. Sci.* **1994**, *304*, 3434.
- Lindan, P. J. D.; Harrison, N. M.; Holender, J. M.; Gillan, M. J. *Chem. Phys. Lett.* **1996**, *261*, 246.
- Podloucky, R.; Steinemann, S. G.; Freeman, A. J. *New J. Chem.* **1992**, *16*, 1139.
- Orlando, R.; Pisani, C.; Ruiz, E.; Sautet, P. *Surf. Sci.* **1992**, *275*, 482.
- Anchell, J. L.; Hess, A. C. *J. Phys. Chem.* **1996**, *100*, 18317.
- Nygren, M. A.; Gay, D. H.; Catlow, C. R. A. *Surf. Sci.* **1997**, *380*, 113.
- Sauer, J.; Ugliengo, P.; Garrone, E.; Saunders, V. R. *Chem. Rev.* **1994**, *94*, 2095.
- Hobza, P.; Sauer, J.; Morgenev, C.; Hurych, J.; Zahradnik, R. *J. Phys. Chem.* **1981**, *85*, 4061.
- Sauer, J.; Zahradnik, R. *Int. J. Quantum Chem.* **1984**, *26*, 793.
- Ugliengo, P.; Saunders, V.; Garrone, E. *J. Phys. Chem.* **1990**, *94*, 2260.
- Stefanovich, E. V.; Truong, T. N. *J. Chem. Phys.* **1997**, *106*, 7700.
- Sawabe, K.; Morokuma, K.; Iwasawa, Y. *J. Chem. Phys.* **1994**, *101*, 7095.
- Pacchioni, G.; Ferrari, A. M.; Márquez, A. M.; Illas, F. J. *Comput. Chem.* **1997**, *18*, 617.
- Johnson, M. A.; Stefanovich, E. V.; Truong, T. N. *J. Phys. Chem. B* **1997**, *101*, 3196.
- Mejias, J. A.; Oviedo, J.; Sanz, J. F. *Chem. Phys.* **1995**, *191*, 133.
- Tomasi, J.; Persico, M. *Chem. Rev.* **1994**, *94*, 2027.
- Truong, T. N.; Stefanovich, E. V. *Chem. Phys. Lett.* **1995**, *240*, 253.
- Truong, T. N.; Stefanovich, E. V. *J. Chem. Phys.* **1995**, *109*, 3709.
- Truong, T. N.; Stefanovich, E. V. *J. Phys. Chem.* **1995**, *99*, 14700.
- Stefanovich, E. V.; Truong, T. N. *Chem. Phys. Lett.* **1995**, *244*, 65.
- Stefanovich, E. V.; Truong, T. N. *J. Chem. Phys.* **1996**, *105*, 2961.
- Truong, T. N.; Nguyen, U. N.; Stefanovich, E. V. *Int. J. Quantum Chem. Symp.* **1996**, *30*, 403.
- Truong, T. N.; Truong, T.-T. T.; Stefanovich, E. V. *J. Chem. Phys.* **1997**, *107*, 1881.
- Stefanovich, E. V.; Boldyrev, A. I.; Truong, T. N.; Simons, J. *J. Phys. Chem. B* **1998**, *102*, 4205.
- Truong, T. N. *Int. Rev. Phys. Chem.*, in press.
- McCarthy, M. I.; Schenter, G. K.; Scamehorn, C. A.; Nicholas, J. B. *J. Phys. Chem.* **1996**, *100*, 16989.
- Berendsen, H. J. C.; Postma, J. P. M.; van Gunsteren, W. F.; Hermans, J. *Intermolecular Forces*; Reidel: Dordrecht, The Netherlands, 1981.
- Alper, H. E.; Levy, R. M. *J. Chem. Phys.* **1989**, *91*, 1242.
- Picaud, S.; Hoang, P. N. M.; Girardet, C. *Surf. Sci.* **1992**, *278*, 339.
- de Leeuw, N. J.; Watson, G. W.; Parker, S. C. *J. Phys. Chem.* **1995**, *99*, 17219.
- Colbourn, E. A. *Defects in Solids—Modern Techniques*; Plenum Press: New York, 1986.
- Tasker, P. W.; Duffy, D. M. *Surf. Sci.* **1984**, *137*, 91.
- Colbourn, E. A.; Kendrick, J.; Mackrodt, W. C. *Surf. Sci.* **1983**, *126*, 550.
- Jorgensen, W. L.; Tirado-Rives, J. *J. Am. Chem. Soc.* **1988**, *110*, 1657.
- Stillinger, F. H. *Science* **1980**, *209*, 451.
- Jorgensen, W. L.; Chandrasekhar, J.; Madura, J. D. *J. Chem. Phys.* **1983**, *79*, 926.
- Johnson, M. A.; Stefanovich, E. V.; Truong, T. N.; Günster, J.; Goodman, D. W. Manuscript in preparation.
- Stefanovich, E. V.; Truong, T. N. *J. Chem. Phys.* **1995**, *102*, 5071.
- Stevens, W. J.; Basch, H.; Krauss, M. *J. Chem. Phys.* **1984**, *81*, 6026.
- Chacon-Taylor, M. R.; McCarthy, M. I. *J. Phys. Chem.* **1996**, *100*, 7610.
- Pascual-Ahuir, J. L.; Silla, E.; Tuñón, I. *J. Comput. Chem.* **1994**, *15*, 1127.
- Franks, F., Ed. *Water: A Comprehensive Treatise*; Plenum Press: New York, 1973; Vol. 3.
- Floris, F.; Tomasi, J. *J. Comput. Chem.* **1989**, *10*, 616.
- Pierotti, R. A. *J. Phys. Chem.* **1963**, *67*, 1840.
- Huron, M. J.; Claverie, P. *J. Phys. Chem.* **1972**, *76*, 2123.
- Henrich, V. E.; Cox, P. A. *The Surface Science of Metal Oxides*; Cambridge University Press: Cambridge, U.K., 1994.
- Tikhomirov, V. A.; Geudtner, G.; Jug, K. *J. Phys. Chem. B* **1997**, *101*, 10398.

- (59) Günster, J.; Liu, G.; Kempter, V.; Goodman, D. W. *J. Vac. Sci. Technol. A* **1998**, *16*, 996.
- (60) Ochs, D.; Maus-Friedrichs, W.; Brause, M.; Günster, J.; Kempter, V.; Puchin, V.; Shluger, A.; Kantorovich, L. *Surf. Sci.* **1996**, *365*, 557.
- (61) Onishi, H.; Egawa, C.; Aruga, T.; Iwasawa, Y. *Surf. Sci.* **1987**, *191*, 479.
- (62) Peng, X. D.; Barteau, M. A. *Langmuir* **1991**, *7*, 1426.
- (63) Peng, X. D.; Barteau, M. A. *Surf. Sci.* **1990**, *233*, 283.
- (64) Frisch, M. J.; Trucks, G. W.; Schlegel, H. B.; Gill, P. M. W.; Johnson, B. G.; Wong, M. W.; Foresman, J. B.; Robb, M. A.; Head-Gordon, M.; Replogle, E. S.; Gomperts, R.; Andres, J. L.; Raghavachari, K.; Binkley, J. S.; Gonzalez, C.; Martin, R. L.; Fox, D. J.; Defrees, D. J.; Baker, J.; Stewart, J. J. P.; Pople, J. A. *Gaussian 92/DFT*, Revision G.3; Gaussian, Inc.: Pittsburgh, PA, 1993.
- (65) Scamehorn, C. A.; Harrison, N. M.; McCarthy, M. I. *J. Chem. Phys.* **1994**, *101*, 1547.
- (66) Heidberg, J.; Redlich, B.; Wetter, D. *Ber. Bunseng-Ges. Phys. Chem.* **1995**, *99*, 1333.
- (67) Xu, C.; Goodman, D. W. *Chem. Phys. Lett.* **1997**, *265*, 341.
- (68) Stirniman, M. J.; Huang, C.; Smith, R. S.; Joyce, S. A.; Kay, B. D. *J. Chem. Phys.* **1996**, *105*, 1295.
- (69) Zhou, X. L.; Cowin, J. P. *J. Phys. Chem.* **1996**, *100*, 1055.
- (70) Kuroda, Y.; Yasugi, E.; Aoi, H.; Miura, K.; Morimoto, T. *J. Chem. Soc., Faraday Trans. 1* **1988**, *84*, 2421.
- (71) Ferry, D.; Glebov, A.; Senz, V.; Suzanne, J.; Toennies, J. P.; Weiss, H. *J. Chem. Phys.* **1996**, *105*, 1697.